Phase 1 Trial of Bi-shRNA STMN1 BIV in Refractory Cancer

Minal Barve[1,2], Zhaohui Wang[3], Padmasini Kumar[4], Christopher M Jay[3], Xiuquan Luo[3], Cynthia Bedell[1], Robert G Mennel[2,5], Gladice Wallraven[4], Francis Charles Brunicardi[6], Neil Senzer[1,3,4], John Nemunaitis[1–4,7] and Donald D Rao[3]

[1]Mary Crowley Cancer Research Centers, Dallas, Texas, USA; [2]Texas Oncology, P.A., Dallas, Texas, USA; [3]Strike Bio, Inc., Dallas, Texas, USA; [4]Gradalis, Inc., Dallas, Texas, USA; [5]Baylor University Medical Center, Dallas, Texas, USA; [6]Department of Surgery, David Geffen School of Medicine at University of California, Los Angeles, California, USA; [7]Medical City Dallas Hospital, Dallas, Texas, USA

Stathmin1 (STMN1) is a microtubule modulator that is expressed in multiple cancers and correlates with poor survival. We previously demonstrated *in vivo* safety of bifunctional (bi) shRNA STMN1 bilamellar invaginated vesicle (BIV) and that systemic delivery correlated with antitumor activity. Patients with superficial advanced refractory cancer with no other standard options were entered into trial. Study design involved dose escalation (four patients/cohort) using a modified Fibonacci schema starting at 0.7 mg DNA administered via single intratumoral injection. Biopsy at baseline, 24/48 hours and resection 8 days after injection provided tissue for determination of cleavage product using next-generation sequencing (NGS) and reverse transcription quantitative polymerase chain reaction (RT-qPCR), 5′ RLM rapid amplification of cDNA ends (RACE) assay. Serum pharmacokinetics of circulating plasmid was done. Twelve patients were entered into three dose levels (0.7, 1.4, 7.0 mg DNA). No ≥ grade 3 toxic effects to drug were observed. Maximum circulating plasmid was detected at 30 seconds with less than 10% detectable in all subjects at 24 hours. No toxic effects were observed. Predicted cleavage product was detected by both NGS (n = 7/7 patients analyzed, cohorts 1, 2) and RLM RACE (n = 1/1 patients analyzed cohort 3). In conclusion, bi-shRNA STMN1 BIV is well tolerated and detection of mRNA target sequence-specific cleavage product confirmed bi-shRNA BIV mechanism of action.

Received 6 October 2014; accepted 12 January 2015; advance online publication 28 April 2015. doi:10.1038/mt.2015.14

INTRODUCTION

Stathmin 1 (STMN1), a protumorigenic protein, is a critical intermediate during signal transduction in modulation and control of microtubule depolymerization and interphase tubulin dimer/polymer partitioning. The process of mitotic spindle formation is a coordinated, balanced interaction between the stabilizing activities of microtubule-associated proteins (XMAP215, EB1), motor proteins (predominantly kinesin, *e.g.*, Eg-5), and plus-end depolymerases including XKCM1, MCAK, and STMN1.[1] A tightly regulated sequenced pattern of STMN1 phosphorylation and dephosphorylation is necessary for entry into prophase and, terminally, into cytokinesis, respectively.[2,3] These functions are critical for malignant cell survival.[4]

STMN1 is highly expressed in a variety of human malignancies,[5–7] and has been shown to be upregulated in multiple cancers.[8–11] Moreover, upregulated stathmin has been shown to be significantly correlated with poor survival.[11–13] High STMN1 expression negatively influences response to microtubule targeting drugs.[14,15] Knockdown of malignant cell STMN1 expression results in an increase in the G2M phase cell population, an inhibition of clonogenicity, and a marked increase in apoptosis.[6,16,17] Furthermore, RNAi-mediated STMN1 knockdown inhibits tumor proliferation and cancer cell invasion in both A549 and H1299 NSCLC lines *in vitro*[18] and tumor growth of MKN-45 gastric cancer *in vivo*.[19]

We previously demonstrated >90% knockdown of STMN1 protein with bi-shRNA STMN1 bilamellar invaginated vesicle (BIV) in comparison to control which correlated *in vitro* (CCL-247 and SK-Mel-28) and *in vivo* (CCL-247) with tumor cell death and nodule regression, respectively.[20,21] Similar results with bi-shRNA BIV therapeutics to other molecular targets have also been demonstrated.[22] Toxicology and biodistribution studies in biorelevant rats and mice predict a high expectation of safety in cancer patients thereby justifying phase 1 study.[21,23]

The bi-shRNA technology has previously been utilized to silence furin expression and consequent TGFβ isoform activation as part of a novel immune modulatory therapeutic, FANG vaccine, now progressing through a series of phase 2 trials.[24–26] Clinical results demonstrate 90–95% TGFβ1 and β2 knockdown.

The delivery mechanism of the bi-shRNA STMN1 vector comprises a 1, 2-dioleoyl-3-trimethylammonium propane and cholesterol liposome.[27–30] This is a manually extruded formulation which forms BIV's, which encapsulate the nucleic acid STMN1 vector thereby forming a fusogenic therapeutic nanolipoplex. Clinical safety and efficacy of these BIVs for DNA vector delivery has been demonstrated in several clinical trials.[23,29] Specifically, DNA delivery following systemic administration to target organ/tissue sites and functionality were demonstrated.[23,30] We seek

Correspondence: John Nemunaitis, Mary Crowley Cancer Research Centers, 12222 Merit Drive, Suite 1500, Dallas, Texas 75251, USA.
E-mail: jnemunaitis@marycrowley.org

to expand the use of this BIV vehicle to systemically deliver bi-shRNA DNA vector to cancer patients. Preliminary to systemic delivery, using intratumoral delivery, we demonstrate functionality and safety of the bi-shRNA STMN1 nanolipoplex in the presence of circulating plasmid.

RESULTS

Twelve patients received one IT injection of bi-shRNA STMN1 BIV and all 12 were evaluable for safety, verification of mechanism, and determination of-response. Demographics of these patients are shown in **Table 1**.

Safety

No grade ≥ 3 drug-related toxic effects were observed. Toxic effects which were possibly or definitely related to bi-shRNA STMN1 BIV are shown in **Table 2**. Four grade < 3 events were interpreted as nonrelated events. These included cellulitis (not at injection site), hypokalemia, superior vena cava syndrome (related to cancer), and cerebral hemorrhage (related to cancer metastasis) within 30 days of study treatment.

Response

Patient response at month 1 and survival are shown in **Table 3**. Twenty percent tumor necrosis on day 8 in comparison to 0% necrosis at baseline was noted in patient 1009.

Pharmacokinetics

Total DNA was extracted from whole blood on all 12 patients at defined time points and analyzed by qPCR. All patients had significant amount of plasmids in the circulation (**Figure 1a**), one patient with angiosarcoma (a highly vascular solid tumor) had higher circulating copies of STMN1 DNA at 1.33×10^9 copies per 100 µl of blood (**Figure 1a**, patient #1002). The highest copies of circulating plasmids detected for other patients ranged from 7.15×10^5 (**Figure 1a**, patient #1004) to 1.51×10^8 (**Figure 1a**, patient #1009) per 100 µl of blood. Typically, PK showed circulating plasmids dropping to less than 10% of the highest copies detected within 5 minutes (patient #1007, **Figure 1b**,**c**; patient #1009, **Figure 1c**). A few patients showed longer initial circulating half-lives (patients # 1009 and #1010, **Figure 1c**); however, in all cases plasmid concentrations decline to less than 10% within 24 hours (**Figure 1c**) and less than 0.1% after 7–8 days (data not shown).

RNA interference mediated cleavage product detection

mRNA target strand cleavage product was identified within the tumor mass on day 1 or 2 postinjection in three of the cohort 1 (patient #1002, 1004, and 1006) and all of the cohort 2 patients as per NGS method (**Figure 2a**). The sample from patient #1005 did not yield sufficient material to pass the quality control used for NGS processing and was therefore not included in the run. For cohort 3, we first used the less sensitive method of gel-electrophoresis analysis to identify RLM-RACE product; the expected cleavage product was readily identified from cohort 3 patient #1013 (**Figure 2b**). The identity of the RLM-RACE product was then sequence confirmed (**Figure 2c**). Cohort 3 samples were not further analyzed by NGS.

Table 1 Patient characteristics

Cohort #	Patient #	Age/ sex	Cancer	Site injected	Dose (mg DNA)[a]	Prior treatment regimen
1	1002	80/F	Angiosarcoma	Arm	0.7, B	Radiotherapy, Tamoxifen, Gemzar + Taxotere, Gemzar + Taxol, Taxol
(IT inj)	1004	60/F	Anal	Labia	0.7, A	Radiotherapy, 5 FU + Mitomycin C, Cisplatin + Gemzar, Irinotecan, Erbitux + Cisplatin + Gemzar, Carbo + Taxol, Carbo + Gemzar
	1005	70 / M	Colorectal	Chest	0.7, A	Eribitus, Oxaliplatin + FU, 5FU+Leucovorin +Avastin, FOLFOX, Xeloda, FOLFIRI + Avastin
	1006	63/F	Ovarian mets	Axillary lymph node	0.7, B	Carboplatin/Paclitaxel, Gemcitabine/Carboplatin, Doxil, ATI-1123, CEP 37250/KJK 2804
2	1007	60/M	Melanoma	Axillary lymph node	1.4, A	Radiotherapy, Interferon, Carboplatin, Taxol, Ipilimumab, DTIC, Vemuvafenib
(IT inj)	1008	50/F	Breast	Breast	1.4, B	Radiotherapy, Tamoxifen, Arimidex + Lupron, Xeloda + Zometa, Vinorelbine, Xeloda + Xgeva
	1009	70/M	Colorectal	Abdomen	1.4, A	Radiotherapy, Avastin, 5FU, Oxaliplatin, Leucovorin, MLN 9708, Stivarga
	1010	50/F	Breast	Chest	1.4, B	Radiotherapy, Acid Ceramide, Taxol, Carbo + Gemzar, Anaztrozole
3	1011	56/F	Lymphoma	Right inguinal node	2.0, A	R-CVP, T0926, Tyrosine Kinase Inhibitor
(IT inj)	1012	77/M	Melanoma	Left inguinal nodule	2.0, B	None
	1013	61/F	Ovarian	Left axillary node	2.0, A	Carboplatin, Taxol, Taxotere, Cisplatin, Doxil, Gemcitabine, Paclitaxel, Custirsen
	1017	58/F	Melanoma	Left inguinal nodule	2.0, B	Interferon, Cavatak

[a]Group A = 24-hour biopsy; Group B = 48-hour biopsy.

Table 2 Toxic events possibly-definitely related to bi-shRNA STMN1 BIV

Preferred term	CTC grade	Relationship to study drug	Number of events	Number of subjects
General disorder, other: achiness	1	Possibly related	1	1
General disorder, other: night sweats	1	Possibly related	1	1
Hypokalemia	2	Possibly related	1	1
Injection site reaction	1	Definitely related	1	1
Lymph node pain	1	Possibly related	1	1
Pain	1	Possibly related	1	1

CTC, common toxicity criteria.

Table 3 Clinical response

Patient ID	Cohort	Dose	Survival status	Days since treatment start	Response month 1 SD/PD
1002	1	0.7 mg	Dead	81	SD
1004	1	0.7 mg	Dead	510	SD
1005	1	0.7 mg	Dead	482	SD
1006	1	0.7 mg	Alive	642	SD
1007	2	1.4 mg	Alive	601	SD
1008	2	1.4 mg	Dead	257	SD
1009	2	1.4 mg	Dead	208	SD
1010	2	1.4 mg	Dead	22[a]	
1011	3	2 mg	Alive	322	SD
1012	3	2 mg	Alive	279	SD
1013	3	2 mg	Alive	279	SD
1017	3	2 mg	Alive	76	SD

[a]Patient 1010 was admitted to the hospital for superior vena cava (SVC) syndrome secondary to metastatic breast cancer on 22 February 2013. A chest x-ray performed on 23 February 2013 showed progression of pulmonary metastasis. She was unable to lay flat for simulation or to even start radiation therapy. She was admitted for further treatment and monitoring to try and start radiation. The SVC syndrome stabilized enough to receive radiation therapy. The patient was discharged as stable on 01 March 2013 and still receiving radiation. The SVC syndrome stabilized, but never resolved. The patient was admitted to the hospital on 08 March 2013 due to worsening dyspnea and extreme fatigue. The patient's disease ultimately continued to progress and the patient passed away.

STMN1 mRNA expression

RT-qPCR data were normalized to glyceraldehyde-3-phosphate dehydrogenase mRNA level by ΔΔCt method and further compared to the STMN1 level in cultured HCT-116 cells (**Figure 3**). The STMN1 mRNA expression level for patient 1002 was higher than in HCT-116 at pretreatment (**Figure 3**, 1002_BL), STMN1 mRNA level dropped to lower level two days post-treatment (**Figure 3**, 1002_D3) and returned to the initial level 6 days post-treatment (**Figure 3**, 1002_D7). STMN1 mRNA level for patient 1006 was too low to assess knockdown effect. Both patients 1011 and 1013 data showed effective reduction of STMN1 mRNA at day 2 post-treatment (**Figure 3**, 1011_D2 and 1013_D2). Similarly, the STMN1 mRNA level for patients 1011 and 1013 returned to baseline level. During RNA analysis, patient 1012's sample was identified as heavily stained with melanin (brown color) and was excluded from analysis (melanin is a known inhibitor of DNA polymerase). Insufficient tissue was available to determine protein expression response.

DISCUSSION

This study demonstrates the safety of intratumoral administration of bi-shRNA STMN1 BIV at dose levels between 0.7 and 2.0 mg pDNA. Furthermore, demonstration of circulating pDNA up to 1.3×10^9 copies per 100 ìl blood, with no evidence of concurrent or 30-day toxic effect, supports justification of i.v. administration starting at dosing levels calculated to produce the range of circulating plasmid levels herein documented. This study was not designed to evaluate tumor response, thus no conclusion regarding response to a single intratumoral injection can be reached. The focus of this evaluation was to verify bi-shRNA STMN1 mechanism of action as reflected in the detection of mRNA targeted sequence-specific cleavage product. These fragments are not normally expressed in biopsied tumor tissue as there is no natural RNAi cleavage to the designed STMN1 sequence site. Here, we demonstrate the bi-shRNA^{STMN1} specific cleavage product is found in all cohort 1 and 2 treated tissues examined with the highly sensitive NGS method. The NGS counts on the specific cleaved STMN1 mRNA varied widely from tissue to tissue possibly due to the varied abundance of tumor cells and inhomogeneity of STMN1 mRNA expression within the sampled tissue. For patient 1013 of cohort 3, the specific cleavage product was found in treated tissue one day after the treatment with a less sensitive RLM-RACE method.

The RT-qPCR method also demonstrated reduced target mRNA expression within the treated tissue samples further validating efficacy and specificity of the therapeutic agent. Our formulation appears to be safe within the pDNA range detected in circulation; the highest detected pDNA at 1.3×10^9 copies pDNA per 100 µl is equivalent to 0.004 mg/kg in an average 70 kg person. Within the dose range used in this study, we were able to readily demonstrate one of the mechanisms of drug action (target mRNA cleavage) and the result of drug treatment at molecular level (reduction of target mRNA). mRNA PK showed that the target mRNA was effectively reduced within 1–2 days after the treatment and then back to a normal level after 7–8 days post-treatment, this is very similar to what we observed *in vitro*.[20] To achieve clinical effectiveness, we believe the treatment schedule will need to be dosed two times per week in order to continuously silence target gene expression as the intended therapeutic effect. The other mechanisms of action of bi-shRNA, *i.e.*, p-body sequestration, noncleavage dependent DNA degradation and inhibition of translation,[20] were not evaluated.

A variety of target specific anti-stathmin effectors including ribozymes[32] and si-RNA[6,16] have been used to silence STMN1 *in vitro*[2,16,32] and, additionally, in combination with chemotherapeutic agents where additive to synergistic interactions have been demonstrated, but prior to this report no evidence of cleavage product confirmation has been demonstrated.[33–35] Previously, we have described bi-shRNA STMN1 BIV cleavage product detection both *in vitro* and *in vivo*, but not in patients.[21] Data presented in this report are the first demonstration that STMN1 expression can be knocked down by RNAi approach in humans. Further clinical studies could advance this therapeutic modality into an effective

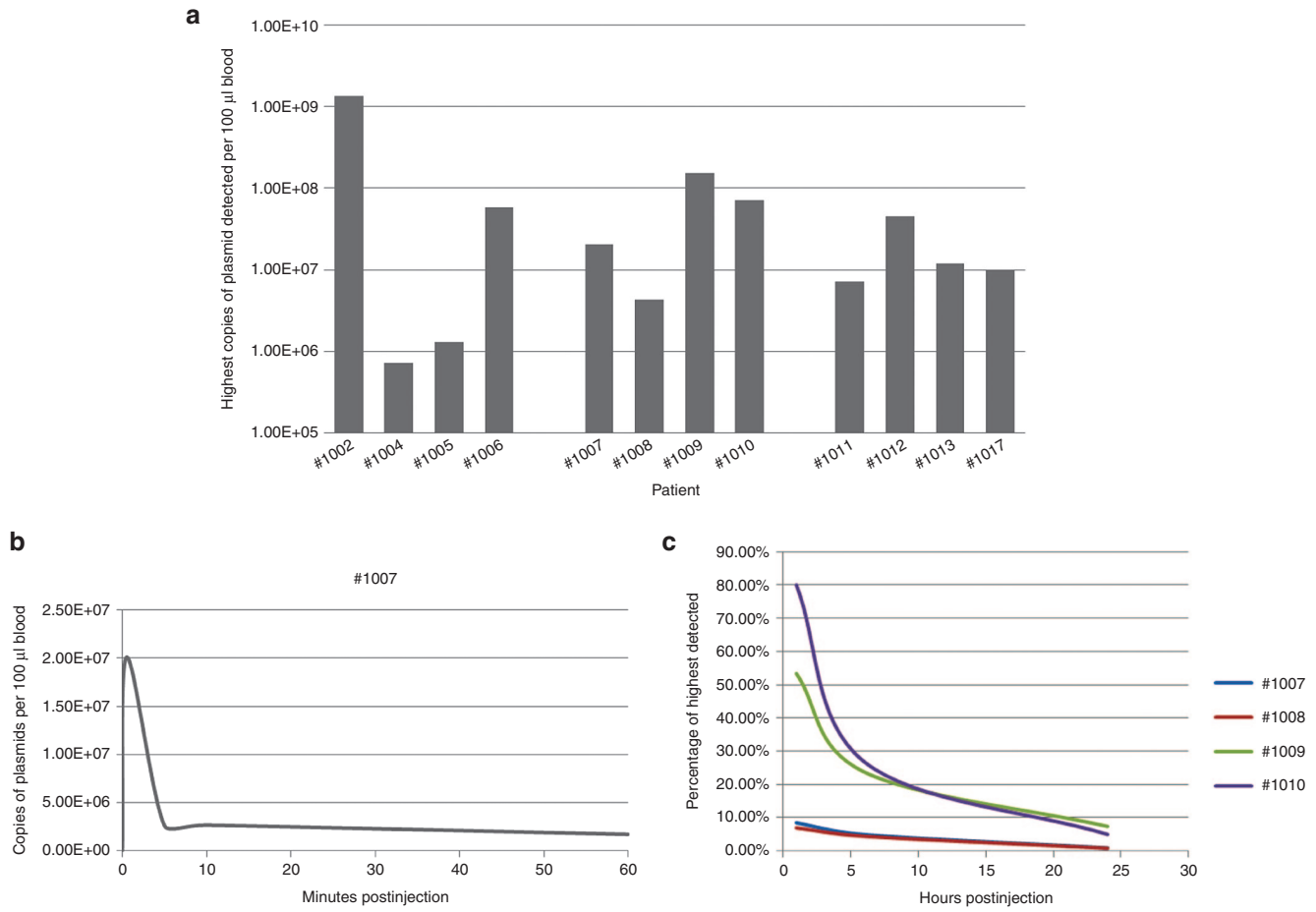

Figure 1 Whole blood pharmacokinetics of bi-shRNA STMN1. Blood was collected at a distal location away from the intratumoral injection site at defined time points. Hundred microliters of whole blood were extracted for DNA. Hundred nanograms of each sample were analyzed by quantitative polymerase chain reaction for the presence of bi-shRNA STMN1. The detected plasmid was normalized to the total DNA extracted per 100 µl of blood sample. Panel (**a**) shows the highest copies of plasmids detected from each patient's time course samples. Panel (**b**) shows a typical pharmacokinetics within 1 hour postinjection (patient #1007). Panel (**c**) shows the pharmacokinetics of cohort 2 patient samples between 1 hour and 24 hours postinjection.

cancer therapeutic agent either as stand alone or in combination with chemotherapeutic agents.

Constitutively expressed shRNA using a pol II promoter on a miR-30 backbone mimics a pri-miRNA and potentially provides an advantage over synthetic siRNA by utilizing the full array of the endogenous miRNA biogenic machinery. Using an adapted stem-loop reverse transcription-polymerase chain reaction RT-PCR method,[36] we previously confirmed the presence of the predicted guide strand *in vivo*.[20] We were able to[20] amplify the guide strand sequence from RNA isolated from cells transfected with either bi-shRNA STMN1 or siRNA^{STMN1}.

Studies on the synthesis and maturation of miRNAs provided guidance on the design of shRNA.[37–39] With respect to delivery other liposomes are routinely transported into target cells by clathrin-mediated endocytosis and/or macropinocytosis, processes resulting in low efficiency of endosome release into the cytoplasm.[40,41] In contradistinction, the fusogenic BIVs utilized here bypass endosomal/lyzosomal encapsulation thereby allowing for more effective intracellular delivery. In addition, avoiding the use of double-stranded RNA moieties (siRNA and shRNA, respectively) and bypassing endosome transport (with exposure to Toll-like receptors (TLR)) minimizes the risk of interferon mediated off-target side effects (IFN-α and 2′-5′ OAS will be evaluated in the phase 1, 4 bi-shRNA STMN1 study).

In a comparison of the functional effectiveness of identical target strand-specific sequence bi-shRNA STMN1 to siRNA^{STMN1} in a HCT-116 growth inhibition assay, we generated dose response curves showing greater cell kill with the bi-shRNA STMN1. Although bi-shRNA superior effectiveness was shown throughout the full comparison dose range, the target specific cleavage product (5′ rapid amplification of cDNA ends (5′-RACE)) was detected at all siRNA^{STMN1} concentrations, but only at the higher dose of bi-shRNA STMN1. Thus, although cleavage product can be used as a measure of bi-shRNA STMN1function, the multiple mechanisms of bi-shRNA are not limited to just the RISC cleavage dependent component.

In conclusion, bi-shRNA STMN1 BIV is safe at low intratumoral injected dose levels achieving measurable serum plasmid levels out to 6 hours on the basis of which additional bi-shRNA STMN1 BIV testing has been initiated to explore safety and activity of intravenous delivery; the final results of which will be reported when completed. Importantly, we were able to

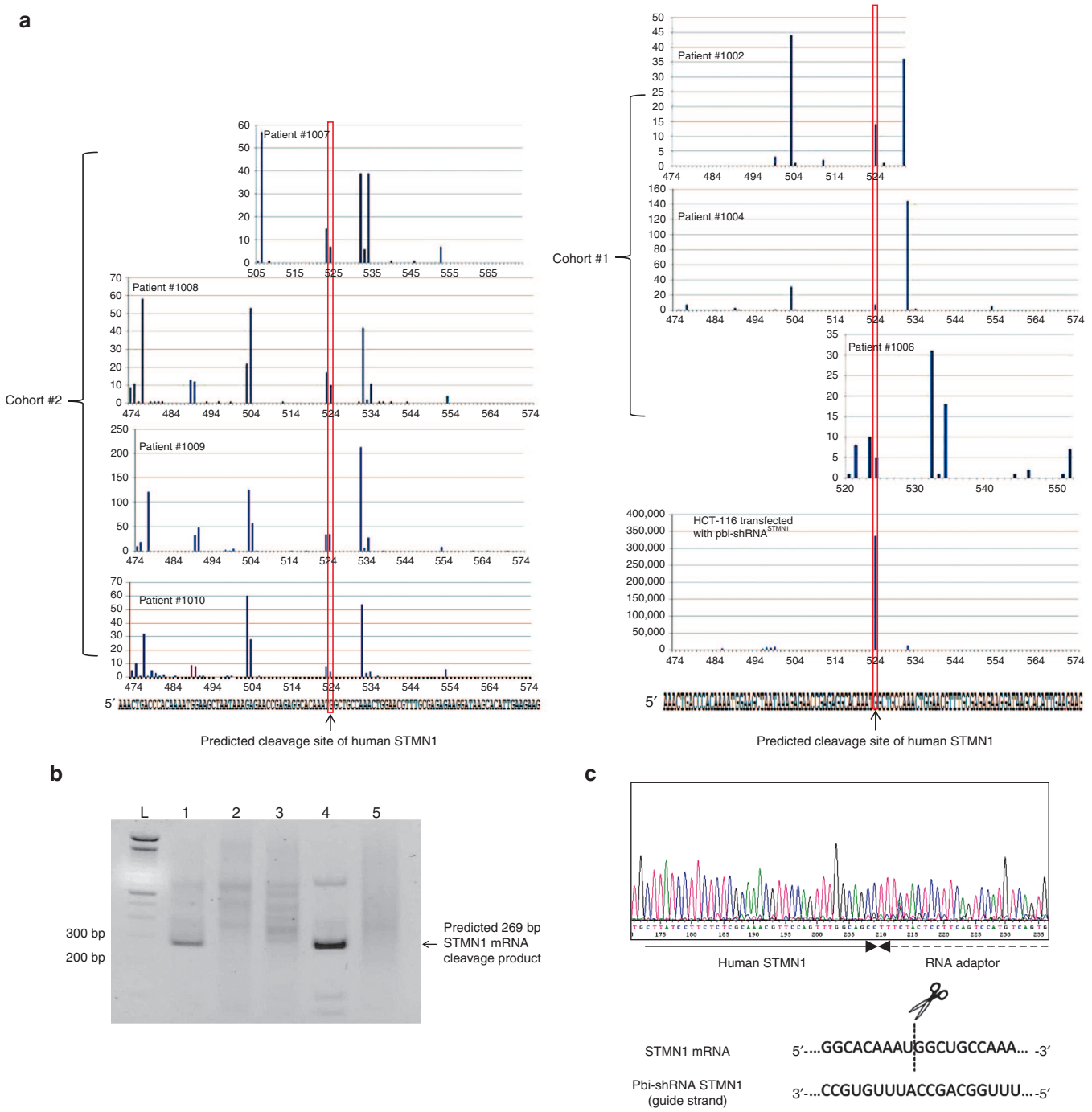

Figure 2 Demonstrate mechanism of drug action: detection and identification of RNAi-mediated target mRNA cleavage product. RNA ligase-mediated RACE (RLM-RACE) and next-generation sequencing (NGS) were employed to identify RNAi-mediated target mRNA cleavage in human tumors with intratumoral injections of bi-shRNA STMN1 BIV. Total RNA were extracted from needle biopsies of patient tumor and analyzed for the presence of RNAi mediated cleavage product. (**a**) Sequence alignment of NGS data on treated tumor samples from cohort 1 patients and HCT-116 cells treated with bi-shRNA STMN1 for positive control (right panel), and from cohort 2 patients (left panel). Red rectangular boxes indicate the correct cleavage product. (**b**) A 4% agarose gel image of RLM-RACE analysis on tumor biopsy samples from patient #1013. Lane L is 100 bp DNA size marker, lane 1 is HCT-116 cells treated with bi-shRNA STMN1, lane 2 is HCT-116 cells without treatment, lane 3 is patient #1013 pretreatment sample, lane 4 is patient #1013 24 hours post-treatment biopsy, lane 5 is patient #1013 day 7 post-treatment sample. Arrow indicates the correct 269 bp cleavage product band, the correct size band was sequence confirmed. (**c**) A representative sequence chromatograph of the STMN1 cleavage product. The broken arrow indicates the RNA adaptor which was used to ligate the cleavage product. The filled arrow indicates human STMN1 sequence. A diagram illustrates the RNAi-mediated cleavage site of human STMN1 mRNA.

demonstrate clear evidence of bi-shRNA function by the detection of targeted-sequence cleavage product via both NGS and RT PCR methods. These findings, coupled with efficient packaging and intracellular delivery in a clinically effective systemic delivery fusogenic nanolipoplex[23,29] provide the basis for the clinical entry of a systemic RNAi therapeutic.

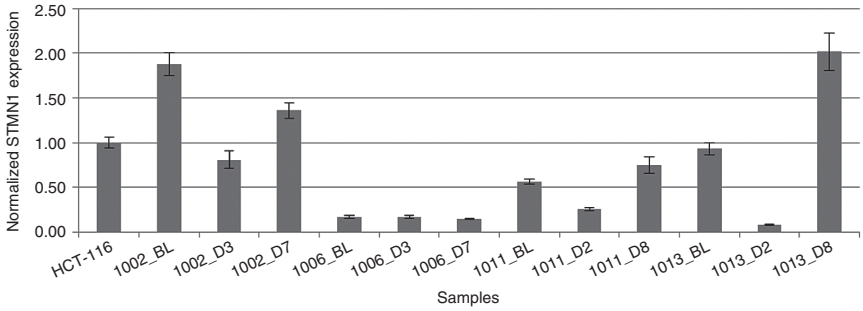

Figure 3 Target gene knockdown assessment by reverse transcription quantitative polymerase chain reaction (RT-qPCR). Normalized STMN1 mRNA level with RNA isolated from biopsy samples of patients 1002, 1006, 1011, and 1013. RT-qPCR was normalized to GAPDH by ΔΔCt method. Triplicates were performed for each RT-qPCR and compared to STMN1 mRNA level in HCT-116 cells. Each sample is designated by patient number and biopsy harvest time. BL, base line; D3, day 3 postinjection; D2, day 2 postinjection; D7, day 7 postinjection; D8, day 8 postinjection. GAPDH, glyceraldehyde-3-phosphate dehydrogenase

MATERIALS AND METHODS

Inclusion criteria. All patients were treated at Mary Crowley Cancer Research Centers, Dallas, TX. Patients were eligible for inclusion in this study if they met the following key criteria: (i) histologically confirmed advanced and/or metastatic cancer; (ii) biopsy accessible lesion; (iii) subjects that have completed all acceptable therapies; (iv) age ≥18 years; (v) ECOG performance status (PS) 0–2; (vi) adequate organ and marrow function; (vii) signed IRB approved informed consent; and (viii) negative pregnancy test. Patients were excluded from this study for the following selected reasons: (i) cancer treatment within 3 weeks prior to entering the study; (ii) patients with known active brain metastases; and (iii) other medical disorders (Hepatitis B and C infection, human immunodeficiency virus, autoimmune disease).

Study design. This study design was (i) to determine single dose safety over 1 month, (ii) to obtain evidence of plasmid circulation, and (iii) to verify bi-shRNA mechanism via cleavage product detection.

Patients were accrued in four-patient, dose-escalation cohorts using a modified Fibonacci schema (100%→50%→33%→33%) at a starting intratumoral dose of 0.7 mg (equivalent to 0.010 mg/kg in a 70 kg human) of DNA up to a dose of 2.0 mg (equivalent to 0.029 mg/kg in a 70 kg human) of DNA intratumoral/single dose. Patients enrolled into Cohort 1 were staggered. No patient received the study agent until the preceding subject received the first injection plus an additional week of follow up. The bi-shRNA STMN1 BIV was administered as described below (see Injection Technique). Tumor staging (by comprehensive computed tomography/magnetic resonance imaging scans) was performed at baseline and at end of treatment. Each patient was monitored closely for toxicity throughout the study. If one of four subjects within a dose cohort experienced a DLT, that dose cohort would be expanded to six patients provided no further subjects experienced a DLT. If no further subjects experienced a DLT, dose-escalation was allowed to continue. If ≥2 subjects within a dose cohort experienced a DLT, that would define the DLT dose level and the maximum tolerated dose would be designated the penultimate dose level.

Serum for pharmacokinetics (PK) was collected within 30 minutes prior to administration and at the following time points afterwards: ≤30 seconds (*i.e.*, immediately after administration drawn from a separate site), 5 minutes, 30 minutes, 1 hour, 6 hours, 24 hours, 48 hours, and on day 8. One to 2 weeks prior to the treatment, a biopsy of the accessible lesion was obtained for reverse transcription quantitative polymerase chain reaction (RT-qPCR), 5′ RLM RACE (bi-shRNA STMN1 expression and target strand sequence specificity), next-generation sequencing (NGS), and plasmid baseline assays (bi-shRNA STMN1 delivery). Additionally, using a randomized approach, a biopsy of an accessible tumor lesion was obtained at 24 hours (± 2 hours) postinfusion in three patients and at 48 hours postinfusion in the remaining three patients for (including but not limited to) RT-qPCR (STMN1 mRNA expression), RLM 5′ RACE (bi-shRNA STMN1efficacy), NGS, and plasmid baseline assays (bi-shRNA STMN1 delivery)[30] and (if possible) stathmin protein assessment. The entire lesion was excised or incisionally biopsied on day 8, 7 days postadministration for immunohistochemistry, H&E, plasmid qPCR, RACE, NGS, and (if possible) stathmin protein assessment.

Lipoplex/DNA products in general may induce an inflammatory response. Therefore immediately prior to injection subjects were premedicated with oral dexamethasone (8 mg, 1 hour prior to injection), indocin (25 mg) and acetaminophen (650 mg).[31] The night before injection, subjects were premedicated with 8 mg of oral dexamethasone. All patients not already taking a proton pump inhibitor received rabeprazole sodium 20 mg po qd 24 hours prior to study drug and continuing for 5 days.

Injection technique. In all patients, the longest diameter of the tumor was determined and trisected. At each of the two trisection points the needle was inserted perpendicular to the skin and *a minimum* of 0.5 ml of bi-shRNA STMN1 BIV injected into each site. The remainder of the volume (*i.e.*, > 1 ml) was equally divided and injected by a fanning technique through each of the two individual injection sites. A Tegaderm dressing (3M Healthcare, St. Paul, MN) was adhered to the tumor/injection site and the tumor, perpendicular diameter, and injection sites marked for biopsies.

PK analysis. Blood samples were collected from patients at defined time points (baseline, within 0.5, 5, 30, 60 minutes, 6 hours, 1 and 2 days following injection) for PK analysis. The blood was collected in ethylenediaminetetraacetic acid tubes, aliquotted, and frozen until ready for analysis. Total DNA was extracted from 100 µl whole blood using the QiaAmp extraction kit (Qiagen, Valencia, CA). Extracted DNA was quantified by NanoDrop (Thermo Scientific, Wilmington, DE). Quantitative PCR was performed using reagents from Applied Biosystems and the Applied Biosystems 7900HT Fast Real-Time PCR instrument (Life Technologies, Grand Island, NY). Positive control bi-shRNA STMN1 plasmid DNA was used to generate standard curves and the patient samples were quantified relative to the standard. Each sample was tested in triplicate and the raw qPCR results (copies of bi-shRNA STMN1 plasmid) were normalized relative to the total yield of DNA extracted from each respective blood sample. DNA extraction and qPCR were done by GE/SeqWright (Houston, TX).

Tumor biopsies. Core needle biopsies were collected from enrolled patients at pretreatment, 24 or 48 hours, and 7 or 8 days after a single intratumoral injection. A core biopsy was divided into five parts: one part was embedded in neutral buffered formalin, two parts were stored in optimum cutting temperature compound medium, and the remaining two parts were submerged in a tube containing Allprotect tissue reagent

(Qiagen). Samples stored in Allprotect tissue reagent were transported on wet ice, kept at a 4 °C refrigerator overnight and then stored at −20 °C until use.

Nucleic acid isolation from tumor biopsies. Total RNA was extracted from tumor biopsies for RLM-RACE assay. AllPrep DNA/RNA/Protein mini kit (Qiagen) was used to isolate DNA, RNA, and protein from the cohort 1 and 2 tumor biopsies. DNA/RNA/protein isolation was essentially done by following the procedures recommend by the manufacturer; briefly, 10–30 mg of tumor biopsies was homogenized in RLT buffer provided by the kit. The homogenate was then loaded onto an Allprep DNA spin column. The total DNA (including genomic DNA and plasmid DNA) was bound to the DNA spin column and was eluted using EB buffer. The flow-through after passing through the DNA spin column was precipitated using ethanol and then loaded to an RNeasy column. The total RNA bound to the RNeasy column was eluted in nuclease-free water. The flow-through after passing through the RNeasy column was precipitated using APP buffer and dissolved in 4% SDS buffer. The isolated total DNA and RNA were quantified using NanoDrop (Thermo Scientific). The integrity of total RNA was examined on a RNA chip using Experion automated electrophoresis system (Bio-Rad, Hercules, CA). In order to improve RNA extraction yield, 1 ml Trizol (Life Technologies) was used to homogenize 10–30 mg tumor biopsies of the third cohort. After centrifugation, the aqueous phase was precipitated using isopropanol. The isolated total RNA was then treated with DNase I (Qiagen) and cleaned-up using an RNeasy column (Qiagen). The isolated total RNA was quantified using Nanorop (Thermo Scientific). The integrity of total RNA was examined on a RNA chip using Experion automated electrophoresis system (Bio-Rad)

RLM-RACE. Three to six micrograms of total RNA were ligated to 250 ng of an RNA adaptor at 37 °C for an hour. The ligated RNA was purified using Amicon Centrifugal Filter Unit (100 KDa) (Millipore, Billerica, MA) and was then applied to synthesize cDNA using STMN1-specific RT primer and a SuperScript III reverse transcriptase kit (Life Technologies). A portion of the synthesized cDNA was used as templates in a 50 µl of PCR amplification reaction primed with the RNA adaptor-specific primer and STMN-specific primers (Platinum Taq DNA polymerase kit, Life Technologies). An additional round of PCR with nested primers was performed to amplify the signals of site-specific STMN1 cleavage product. The PCR products were visualized on a 2% E-gel (Life Technologies). The band with predicted size was cut from the gel, purified using a QIAquick gel-purification kit (Qiagen) and sequence-confirmed.

NGS. The nested-PCR products of RLM-RACE were analyzed using NGS performed by GE/SeqWright (Houston, TX). Briefly, the nested-PCR products were quantified using PicoGreen and quality-checked on an agarose gel. Pair-ended and coded libraries were generated for each sample using a TruSeq DNA sample preparation kit (Illumina, San Diego, CA). The libraries were then combined at equal molar ratios and sequenced on an Illumina MiSeq System with 2 × 250 bp read lengths. The sequencing run was spiked with 50% Phi X control to increase diversity and data quality. The Illumina MiSeq sequencing reads underwent alignment to human STMN1 transcript (GenBank accession number NM_203401) and were analyzed for predicted STMN1 cleavage site. Cutadapt (v 1.2.1) was used to trim off the RNA adaptor sequence (Martin M. 2011) and Tophat (v 2.0.6) was employed to align the trimmed reads against the reference sequence with perfect match.

ACKNOWLEDGMENTS

We gratefully acknowledge the generous support of the Summerfield G. Roberts Foundation, the Crowley-Carter Foundation, the Crowley Shanahan Foundation, the Marilyn Augur Family Foundation, W.W. Caruth Jr. Foundation Fund of the Communities Foundation of Texas, the Merkle Family Foundation, and Gradalis, Inc. The following authors are shareholders in Gradalis, Inc.: Z.W., P.K., C.J., G.W., F.C.B., N.S., J.N., and D.D.R. The authors have no other relevant affiliations or financial involvement with any organization or entity with a financial interest in or financial conflict with the subject matter or materials discussed in the manuscript.

REFERENCES

1. Niethammer, P, Kronja, I, Kandels-Lewis, S, Rybina, S, Bastiaens, P and Karsenti, E (2007). Discrete states of a protein interaction network govern interphase and mitotic microtubule dynamics. *PLoS Biol* **5**: e29.
2. Iancu-Rubin, C, Nasrallah, CA and Atweh, GF (2005). Stathmin prevents the transition from a normal to an endomitotic cell cycle during megakaryocytic differentiation. *Cell Cycle* **4**: 1774–1782.
3. Gavet, O, Ozon, S, Manceau, V, Lawler, S, Curmi, P and Sobel, A (1998). The stathmin phosphoprotein family: intracellular localization and effects on the microtubule network. *J Cell Sci* **111 (Pt 22)**: 3333–3346.
4. Belletti, B and Baldassarre, G (2011). Stathmin: a protein with many tasks. New biomarker and potential target in cancer. *Expert Opin Ther Targets* **15**: 1249–1266.
5. Nemunaitis, J, Senzer, N, Khalil, I, Shen, Y, Kumar, P, Tong, A *et al.* (2007). Proof concept for clinical justification of network mapping for personalized cancer therapeutics. *Cancer Gene Ther* **14**: 686–695.
6. Alli, E, Yang, JM and Hait, WN (2007). Silencing of stathmin induces tumor-suppressor function in breast cancer cell lines harboring mutant p53. *Oncogene* **26**: 1003–1012.
7. Nishio, K, Nakamura, T, Koh, Y, Kanzawa, F, Tamura, T and Saijo, N (2001). Oncoprotein 18 overexpression increases the sensitivity to vindesine in the human lung carcinoma cells. *Cancer* **91**: 1494–1499.
8. Jeon, TY, Han, ME, Lee, YW, Lee, YS, Kim, GH, Song, GA *et al.* (2010). Overexpression of stathmin1 in the diffuse type of gastric cancer and its roles in proliferation and migration of gastric cancer cells. *Br J Cancer* **102**: 710–718.
9. Hsu, HP, Li, CF, Lee, SW, Wu, WR, Chen, TJ, Chang, KY *et al.* (2014). Overexpression of stathmin 1 confers an independent prognostic indicator in nasopharyngeal carcinoma. *Tumour Biol* **35**: 2619–2629.
10. Zheng, P, Liu, YX, Chen, L, Liu, XH, Xiao, ZQ, Zhao, L *et al.* (2010). Stathmin, a new target of PRL-3 identified by proteomic methods, plays a key role in progression and metastasis of colorectal cancer. *J Proteome Res* **9**: 4897–4905.
11. Salvesen, HB, Carter, SL, Mannelqvist, M, Dutt, A, Getz, G, Stefansson, IM *et al.* (2009). Integrated genomic profiling of endometrial carcinoma associates aggressive tumors with indicators of PI3 kinase activation. *Proc Natl Acad Sci USA* **106**: 4834–4839.
12. Trovik, J, Wik, E, Stefansson, IM, Marcickiewicz, J, Tingulstad, S, Staff, AC *et al.*; MoMaTec Study Group. (2011). Stathmin overexpression identifies high-risk patients and lymph node metastasis in endometrial cancer. *Clin Cancer Res* **17**: 3368–3377.
13. Ke, B, Wu, LL, Liu, N, Zhang, RP, Wang, CL and Liang, H (2013). Overexpression of stathmin 1 is associated with poor prognosis of patients with gastric cancer. *Tumour Biol* **34**: 3137–3145.
14. Carr, JR, Park, HJ, Wang, Z, Kiefer, MM and Raychaudhuri, P (2010). FoxM1 mediates resistance to herceptin and paclitaxel. *Cancer Res* **70**: 5054–5063.
15. Su, D, Smith, SM, Preti, M, Schwartz, P, Rutherford, TJ, Menato, G *et al.* (2009). Stathmin and tubulin expression and survival of ovarian cancer patients receiving platinum treatment with and without paclitaxel. *Cancer* **115**: 2453–2463.
16. Zhang, HZ, Wang, Y, Gao, P, Lin, F, Liu, L, Yu, B *et al.* (2006). Silencing stathmin gene expression by survivin promoter-driven siRNA vector to reverse malignant phenotype of tumor cells. *Cancer Biol Ther* **5**: 1457–1461.
17. Iancu, C, Mistry, SJ, Arkin, S, Wallenstein, S and Atweh, GF (2001). Effects of stathmin inhibition on the mitotic spindle. *J Cell Sci* **114**(Pt 5): 909–916.
18. Nie, W, Xu, MD, Gan, L, Huang, H, Xiu, Q and Li, B (2015). Overexpression of stathmin 1 is a poor prognostic biomarker in non-small cell lung cancer. *Lab Invest* **95**: 56–64.
19. Akhtar, J, Wang, Z, Zhang, ZP and Bi, MM (2013). Lentiviral-mediated RNA interference targeting stathmin1 gene in human gastric cancer cells inhibits proliferation *in vitro* and tumor growth in vivo. *J Transl Med* **11**: 212.
20. Rao, DD, Maples, PB, Senzer, N, Kumar, P, Wang, Z, Pappen, BO *et al.* (2010). Enhanced target gene knockdown by a bifunctional shRNA: a novel approach of RNA interference. *Cancer Gene Ther* **17**: 780–791.
21. Phadke, AP, Jay, CM, Wang, Z, Chen, S, Liu, S, Haddock, C *et al.* (2011). *In vivo* safety and antitumor efficacy of bifunctional small hairpin RNAs specific for the human Stathmin 1 oncoprotein. *DNA Cell Biol* **30**: 715–726.
22. Liu, SH, Rao, DD, Nemunaitis, J, Senzer, N, Zhou, G, Dawson, D *et al.* (2012). PDX-1 is a therapeutic target for pancreatic cancer, insulinoma and islet neoplasia using a novel RNA interference platform. *PLoS One* **7**: e40452.
23. Jay, C, Nemunaitis, G, Nemunaitis, J, Senzer, N, Hinderlich, S, Darvish, D *et al.* (2008). Preclinical assessment of wt GNE gene plasmid for management of hereditary inclusion body myopathy 2 (HIBM2). *Gene Regul Syst Bio* **2**: 243–252.
24. Senzer, N, Barve, M, Kuhn, J, Melnyk, A, Beitsch, P, Lazar, M *et al.* (2012). Phase I trial of "bi-shRNAi(furin)/GMCSF DNA/autologous tumor cell" vaccine (FANG) in advanced cancer. *Mol Ther* **20**: 679–686.
25. Senzer, N, Barve, M, Nemunaitis, J, Kuhn, J, Melnyk, A, Beitsch, P *et al.* (2013). Long term follow up: phase I trial of "bi-shRNA furin/GMCSF DNA/autologous tumor cell" immunotherapy (FANG™) in advanced cancer. *J Vaccines Vaccin* **4**: 209.
26. Nemunaitis, J, Barve, M, Orr, D, Kuhn, J, Magee, M, Lamont, J *et al.* (2014). Summary of bi-shRNA/GM-CSF augmented autologous tumor cell immunotherapy (FANG™) in advanced cancer of the liver. *Oncology* **87**: 21–29.
27. Templeton, NS, Lasic, DD, Frederik, PM, Strey, HH, Roberts, DD and Pavlakis, GN (1997). Improved DNA: liposome complexes for increased systemic delivery and gene expression. *Nat Biotechnol* **15**: 647–652.

28. Ramesh, R, Saeki, T, Templeton, NS, Ji, L, Stephens, LC, Ito, I *et al.* (2001). Successful treatment of primary and disseminated human lung cancers by systemic delivery of tumor suppressor genes using an improved liposome vector. *Mol Ther* **3**: 337–350.
29. Lu, C, Stewart, DJ, Lee, JJ, Ji, L, Ramesh, R, Jayachandran, G *et al.* (2012). Phase I clinical trial of systemically administered TUSC2(FUS1)-nanoparticles mediating functional gene transfer in humans. *PLoS One* **7**: e34833.
30. Davis, ME, Zuckerman, JE, Choi, CH, Seligson, D, Tolcher, A, Alabi, CA *et al.* (2010). Evidence of RNAi in humans from systemically administered siRNA via targeted nanoparticles. *Nature* **464**: 1067–1070.
31. Barnhart, KJ, Miller, S, Hsu, J, McMannis, J, Smith, P, Abbruzzese, J, Hung, MC. *Systemic Apoptic Gene Therapy for Pancreatic Cancer: Multi-Dose Toxicity Study of the BikDD Nanoparticle*. American Society of Gene & Cell Therapy, Washington, DC, 2010.
32. Mistry, SJ, Benham, CJ and Atweh, GF (2001). Development of ribozymes that target stathmin, a major regulator of the mitotic spindle. *Antisense Nucleic Acid Drug Dev* **11**: 41–49.
33. Mistry, SJ and Atweh, GF (2006). Therapeutic interactions between stathmin inhibition and chemotherapeutic agents in prostate cancer. *Mol Cancer Ther* **5**: 3248–3257.
34. Ngo, TT, Peng, T, Liang, XJ, Akeju, O, Pastorino, S, Zhang, W *et al.* (2007). The 1p-encoded protein stathmin and resistance of malignant gliomas to nitrosoureas. *J Natl Cancer Inst* **99**: 639–652.
35. Wang, R, Dong, K, Lin, F, Wang, X, Gao, P, Wei, SH *et al.* (2007). Inhibiting proliferation and enhancing chemosensitivity to taxanes in osteosarcoma cells by RNA interference-mediated downregulation of stathmin expression. *Mol Med* **13**: 567–575.
36. Soutschek, J, Akinc, A, Bramlage, B, Charisse, K, Constien, R, Donoghue, M *et al.* (2004). Therapeutic silencing of an endogenous gene by systemic administration of modified siRNAs. *Nature* **432**: 173–178.
37. Zeng, Y, Yi, R and Cullen, BR (2005). Recognition and cleavage of primary microRNA precursors by the nuclear processing enzyme Drosha. *EMBO J* **24**: 138–148.
38. Silva, JM, Li, MZ, Chang, K, Ge, W, Golding, MC, Rickles, RJ *et al.* (2005). Second-generation shRNA libraries covering the mouse and human genomes. *Nat Genet* **37**: 1281–1288.
39. Cullen, BR (2005). RNAi the natural way. *Nat Genet* **37**: 1163–1165.
40. Gilleron, J, Querbes, W, Zeigerer, A, Borodovsky, A, Marsico, G, Schubert, U *et al.* (2013). Image-based analysis of lipid nanoparticle-mediated siRNA delivery, intracellular trafficking and endosomal escape. *Nat Biotechnol* **31**: 638–646.
41. Sahay, G, Querbes, W, Alabi, C, Eltoukhy, A, Sarkar, S, Zurenko, C *et al.* (2013). Efficiency of siRNA delivery by lipid nanoparticles is limited by endocytic recycling. *Nat Biotechnol* **31**: 653–658.